Spontaneous parametric down-conversion in periodically poled KTP waveguides and bulk crystals

Marco Fiorentino[1], Sean M. Spillane[1], Raymond G. Beausoleil[1], Tony D. Roberts[2], Philip Battle[2], and Mark W. Munro[2]

[1] *HP Labs, 1501 Page Mill Rd., Palo Alto, California 94304*
[2] *ADVR, 2310 University Way, Bozeman, Montana 59715*
marco.fiorentino@hp.com

Abstract: We present a theoretical and experimental comparison of spontaneous parametric down-conversion in periodically poled waveguides and bulk KTP crystals. We measured a waveguide pair generation rate of $2.9 \cdot 10^6$ pairs/s per mW of pump in a 1-nm band: more than 50 times higher than the bulk crystal generation rate.

© 2007 Optical Society of America

OCIS codes: (270.0270) Quantum optics;(190.4410) Nonlinear optics, parametric processes

References and links

1. P. G. Kwiat, K. Mattle, H. Weinfurter, and A. Zeilinger, "New High-Intensity Source of Polarization-Entangled Photon Pairs," Phys. Rev Lett. **75**, 4337 (1995).
2. P. G. Kwiat, E. Waks, A. G. White1, I. Appelbaum, and P. H. Eberhard, "Ultrabright source of polarization-entangled photons," Phys. Rev. A **60**, R773 (1999).
3. T. B. Pittman, B. C. Jacobs, and J. D. Franson, "Demonstration of Nondeterministic Quantum Logic Operations Using Linear Optical Elements," Phys. Rev. Lett. **88**, 257902 (2002).
4. S. Tanzilli, H. De Riedmatten, H. Tittel, H. Zbinden, P. Baldi, M. De Micheli, D. B. Ostrowsky, N. Gisin, " Highly efficient photon-pair source using periodically poledlithium niobate waveguide," Electron. Lett. **37**, 28, (2001).
5. K. Sanaka, K. Kawahara, and T. Kuga, "New High-Efficiency Source of Photon Pairs for Engineering Quantum Entanglement," Phys. Rev. Lett. 86, 5620 (2001).
6. A. B. U'Ren, C. Silberhorn, K. Banaszek, and I. A. Walmsley, "Efficient Conditional Preparation of High-Fidelity Single Photon States for Fiber-Optic Quantum Networks," Phys. Rev. Lett. **93**, 093601 (2004).
7. D. A. Kleinman, "Theory of Optical Parametric Noise," Phys. Rev. 174, 1027 (1968).
8. K. Koch, E. C. Cheung, G. T. Moore, S. H. Chakmakjian, and J. M. Liu, "Hot Spots in Parametric Fluorescence with a Pump Beam of Finite Cross Section," IEEE J. of Quantum Electron. **31** 769 (1995).
9. P. Baldi, P. Aschieri, S. Nouh, M. De Micheli, D. B. Ostrowsky, D. Delacourt, and M. Papuchon, "Modeling and Experimental Observation of Parametric Fluorescence in Periodically Poled Lithium Niobate Waveguides," IEEE J. of Quantum Electron. **31** 997 (1995).
10. D. F. Walls and G. J. Milburn, "Quantum Optics," (Springer-Verlag, Berlin, 1995).
11. H. Vanherzeele and J. D. Bierlein, "Magnitude of the nonlinear-optical coefficients of $KTiOPO_4$," Opt. Lett. **17** 982 (1992).
12. J. D. Bierlein and H. Vanherzeele, "Potassium titanyl phospate: properties and new applications," J. Opt. Soc. Am. B **6**, 622 (1989).
13. E. C. Cheung, K. Koch, G. T. Moore, J. M. Liu, "Measurements of second-order nonlinear optical coefficients from the spectral brightness of parametric fluorescence," Opt. Lett. **19** 168 (1994).
14. Z. Y. Ou and Y. J. Lu, "Cavity Enhanced Spontaneous Parametric Down-Conversion for the Prolongation of Correlation Time between Conjugate Photons," Phys. Rev. Lett. 83, 2556 (1999).
15. T. E. Murphy, Ph.D. thesis, MIT (2001). See also the pakage for numerically solving the eigenmode problem at `http://www.photonics.umd.edu/software`
16. M. G. Roelofs, A. Suna, W. Bindloss, and J. D. Bierlein, "Characterization of optical waveguides in KTiOP04 by second harmonic spectroscopy," J. Appl. Phys. **9**, 4999 (1994).

#82210 - $15.00 USD Received 18 Apr 2007; revised 24 May 2007; accepted 31 May 2007; published 4 Jun 2007
(C) 2007 OSA

17. T. Kim, M. Fiorentino, P. V. Gorelik and F. N. C. Wong, "Low-cost nanosecond electronic coincidence detector," physics/0501141 (2005).
18. A. B. U'ren, *personal communication*.
19. C. E. Kuklewicz, M. Fiorentino, G. Messin, F. N. C. Wong, and J. H. Shapiro, "High-flux source of polarization entangled photons from a periodically-poled $KTiOPO_4$ parametric downconverter," Phys. Rev. A **69**, 013807 (2004).
20. M. H. Rubin, D. N. Klyshko, Y. H. Shih, and A. V. Sergienko, "Theory of two-photon entanglement in type-II optical parametric down-conversion," Phys. Rev. A **50** 5122 (1994).

1. Introduction

Photon pairs generated using spontaneous parametric down-conversion (SPDC) have been a central ingredient for a number of quantum optics experiments ranging from the generation of entanglement [1, 2] to demonstrations of quantum information processing protocols [3]. The flux of pairs generated by SPDC sources has been steadily growing over the years opening the door to practical applications of correlated and entangled photon pairs.

SPDC sources based on periodically poled waveguides have shown a great potential to generate large numbers of correlated pairs with a few μW of pump [4, 5, 6]. These works, however, lack a clear explanation of the increased pair rate in waveguides and do not directly compare the waveguide result with bulk. Naïvely, field confinement in waveguides is not expected to enhance pair generation rate. Kleinman [7] in a seminal paper on parametric down-conversion noticed that "[SPDC] can not be enhanced by focussing," marking this as one of the distinguishing aspects of SPDC when compared with other nonlinear phenomena such as second harmonic generation. Such behavior can be understood intuitively by noticing that SPDC is a scattering phenomenon that only involves *one* pump photon and therefore does not benefit from higher photon densities created by focussing.

In this paper we derive an explicit formula for the expected pair flux generated by SPDC in waveguides that can be directly compared with the expression for bulk crystals [8]. The derivation also offers important insight into the reason why waveguides enhance pair generation as well as suggesting ways to optimize the generation rate. We set up SPDC experiments in waveguides and bulk to compare the generation rate with the theory and between each other.

2. Theory

The theory of parametric down-conversion in bulk crystals is well established. For a bulk crystal Koch and co-authors [8] calculate the down-converted signal power integrated over all emission angles $d\mathscr{P}_s^{(B)}$ emitted in the frequency (wavelength) interval $d\omega_s$ ($d\lambda_s$). In their calculation Koch *et al.* assume non-collinear emission. In the case of collinear degenerate emission Eq. (39) of Ref. [8] is modified to

$$d\mathscr{P}_s^{(B)} = \frac{\hbar d^2 \mathscr{L} \omega_s^3 \omega_i^2}{\pi c^4 \varepsilon_0 n_p^2 \omega_p} \mathscr{P}_p f(\lambda_s) d\omega_s = (2\pi)^4 \frac{2\hbar c d^2 \mathscr{L} \lambda_p}{\varepsilon_0 n_p^2 \lambda_s^5 \lambda_i^2} \mathscr{P}_p f(\lambda_s) d\lambda_s. \quad (1)$$

Where d is the effective nonlinear coefficient, $\mathscr{L}$ is the crystal length, $\omega_{s,i,p}$ are the signal, idler, and pump frequencies, $\lambda_{s,i,p}$ are the signal idler, and pump wavelengths, c is the speed of light in vacuum, ε_0 is the permittivity of vacuum, n_p is the crystal refractive index at the pump wavelength, and $\mathscr{P}_p$ is the pump power. The function $f(\lambda_s)$ is added to keep into account the collinear geometry and is

$$f(\lambda_s) = \frac{1}{\pi} \int_0^\infty d(r^2) \mathrm{sinc}^2 \left[r^2 + \frac{\mathscr{L}}{2} \gamma(\overline{\omega} - \omega_s) \right]. \quad (2)$$

#82210 - $15.00 USD Received 18 Apr 2007; revised 24 May 2007; accepted 31 May 2007; published 4 Jun 2007
(C) 2007 OSA

Where $\omega_s = 2\pi c/\lambda_s -$ and γ is defined in terms of the derivatives of the phase mismatch Δk,

$$\gamma = \partial_{\omega_s} \Delta k|_{\overline{\omega}} - \partial_{\omega_i} \Delta k|_{\overline{\omega}} \tag{3}$$

and $\overline{\omega}$ is the degenerate frequency for collinear phase matching. Observe that the spectral density in 1 is approximately constant with frequency except for the factor f: for $\omega_s \ll \overline{\omega}$ $f \to 1$ and we recover the result of Ref. [8], for perfectly collinear emission $\omega_s = \overline{\omega}$ and $f = 1/2$. For our simulations it is safe to assume that we are slightly off the perfect collinear condition and take $f = 1$. Note that the signal power in 1 scales linearly with the pump power and crystal length while it is independent of the pump beam shape (although the result was obtained for gaussian beams). The result in Eq. 1 seems to imply that one cannot expect increased signal power by using waveguides with small modes. As we will see this conclusion is not correct once the effects of waveguides are taken into full account.

To obtain an expression for the down-converted signal power for guided modes we will use the same strategy as Ref. [8]. We start with the interaction Hamiltonian due to the nonlinear coupling of signal, idler, and pump. In our semiclassical treatment signal and idler fields are quantized while the pump is a classical field and we neglect its depletion. The nonlinear interaction induces a transition between the ground state (vacuum) and the first excited state (one photon each) of the signal and idler fields. The transition rate is calculated by Fermi's Golden Rule and is used to obtain the power of the emitted signal. Reference [9] reports an expression for the down-converted signal power in a waveguide obtained considering the optical parametric amplification of quantum noise. This method has been criticized in [7] because it requires the use of fictitious input powers. In addition, some of the assumptions used in Ref. [9] are not clearly detailed in the text and this makes a direct comparison with our result hard.

We start quantizing the signal and idler fields following Ref. [10]. We write the monochromatic electric field with frequency $\omega^{(k)}$ as

$$\mathbf{E}_{s,i}(\mathbf{r},t) = i \sum_k \left(c_k u_k(\mathbf{r}) e^{-i\omega^{(k)} t} + c.c. \right) \tag{4}$$

where u_k satisfies the following conditions

$$\left(\nabla^2 + \frac{(\omega^{(k)})^2}{n^2 c^2} \right) u_k = 0 \tag{5}$$

$$\nabla \cdot u_k = 0 \tag{6}$$

$$\int_V u_k^* u_k = 1 \tag{7}$$

The last integral is taken over the quantization volume V. We assume that, for a waveguide, the solution is separable and write

$$u_k(\mathbf{r}) = \frac{1}{\sqrt{L}} U^{(k)}(x,y) e^{i\beta^{(k)} z}, \tag{8}$$

where L is the length of the quantization volume along the propagation axis $\hat{z}$, $\beta^{(k)}$ is the propagation constant, and $\int_A dxdy |U^{(k)}|^2 = 1$ when the integral is carried over the transverse area A of the quantization volume. Observe that $U^{(k)}$ has dimensions of the inverse of a length. The field can be quantized introducing the electric field operator for signal and idler

$$\begin{aligned} \hat{\mathscr{E}}_{s,i} &= \frac{1}{2} \left[\hat{E}_{s,i}(\mathbf{r},t) + \hat{E}_{s,i}^{\dagger}(\mathbf{r},t) \right] \\ &= \frac{i}{2} \sum_k \left[\left(\frac{2\hbar\omega_{s,i}^{(k)}}{n_{s,i}^2 \varepsilon_0} \right)^{1/2} \frac{1}{\sqrt{L}} U_{s,i}^{(k)}(x,y) e^{i(\beta_{s,i}^{(k)} z - \omega_{s,i}^{(k)} t)} \hat{a}_{s,i}^{(i)} + h.c. \right], \end{aligned} \tag{9}$$

#82210 - $15.00 USD Received 18 Apr 2007; revised 24 May 2007; accepted 31 May 2007; published 4 Jun 2007
(C) 2007 OSA

where $n_{s,i}$ are the indexes of refraction for the signal and idler, respectively, and the integration constant is chosen to give the usual commutation rules for the creation and destruction operators. We write the pump field as

$$\begin{aligned}\mathscr{E}_p(\mathbf{r},t) &= \frac{1}{2}\left[E_p(\mathbf{r},t)+E_p^*(\mathbf{r},t)\right]= \\ &= \frac{1}{2}\left[\sqrt{\frac{2\mathscr{P}_p}{cn_p\varepsilon_0}}U_p(x,y)e^{i(\beta_p z-\omega_p t)}+c.c.\right],\end{aligned} \tag{10}$$

were n_p is the refractive index for the pump. We assume $\int dxdy|U_p|^2=1$ and choose the normalization so that when we integrate $\int dxdycn_p\varepsilon_0|E_p|^2/2$ we obtain the pump power $\mathscr{P}_p$. The interaction Hamiltonian is then [8]

$$\hat{H}_I=-\frac{\varepsilon_0}{2}d\int_C\{E_p\hat{E}_s^\dagger\hat{E}_i^\dagger+H.c.\}=\frac{d\sqrt{2}\hbar}{\sqrt{\varepsilon_0 cn_s^2n_i^2n_p}}\frac{\sqrt{\mathscr{P}_p}}{L}\sum_{j,k}\sqrt{\omega_s^{(i)}\omega_i^{(j)}}$$

$$\int_C dxdydz\left[U_p\left(U_i^{(j)}\right)^*\left(U_s^{(k)}\right)^*e^{i(\beta_p-\beta_s^{(k)}-\beta_i^{(j)})z}e^{-i(\omega_p-\omega_s^{(k)}-\omega_i^{(j)})t}\hat{a}_s^{(i)\dagger}\hat{a}_i^{(j)\dagger}+h.c.\right]. \tag{11}$$

Where the integral is calculated over the crystal volume C which has a length $\mathscr{L}$ along the propagation axis and a transverse area A that coincides with the quantization volume transverse section. We can now calculate the matrix element between the initial state $|i\rangle=|00\rangle$ with no photons in the signal and idler modes and the final state $\langle f|=\langle 00|\hat{a}_s^{(l)}\hat{a}_i^{(m)}$ with one photon in each of the modes l and m. By putting $\omega_s^{(l)}=\omega_s$, $\omega_i^{(m)}=\omega_i$, $U_s^{(l)}=U_s$, $U_i^{(j)}=U_i$ and $\Delta k=\beta_p-\beta_i^{(m)}-\beta_s^{(l)}$ and enforcing energy conservation $\omega_p=\omega_s+\omega_i$ we get

$$\begin{aligned}\langle f|\hat{H}_I|i\rangle &= \frac{d\hbar\sqrt{2\mathscr{P}_p\omega_s\omega_i}}{\sqrt{\varepsilon_0 cn_s^2n_i^2n_p}}\frac{1}{L}\int_C dxdydzU_p\left(U_i\right)^*\left(U_s\right)^*e^{i\Delta kz} \\ &= \frac{d\hbar\sqrt{2\mathscr{P}_p\omega_s\omega_i}}{\sqrt{\varepsilon_0 cn_s^2n_i^2n_pL}}\frac{\mathscr{L}}{\sqrt{A_I}}\mathrm{sinc}\left(\frac{\Delta k\mathscr{L}}{2}\right).\end{aligned} \tag{12}$$

Where $A_I=\left(\int_A dxdyU_p\left(U_i\right)^*\left(U_s\right)^*\right)^{-2}$ is the interaction effective area.

To complete our evaluation of the Fermi transition rate we need to write the density of states. For the 1 dimensional state space we are considering the change in the number of signal states $d\mathscr{N}$ for a change dE of the energy is

$$d\mathscr{N}=\frac{L}{2\pi}\frac{n_s}{\hbar c}dE \tag{13}$$

and an analogous relation is valid for the idler. Therefore the density of states is

$$\rho=\frac{L^2}{(2\pi)^2}\frac{n_sn_i}{\hbar c^2}d\omega_s. \tag{14}$$

As it might be expected the density of states is different from the 3 dimensional case used in Ref. [8] (Eq. 9). We apply Fermi's golden rule to get the transition rate

$$\mathscr{W}=\frac{2\pi}{\hbar}\left|\langle f|\hat{H}_I|i\rangle\right|^2\rho=\frac{d^2\mathscr{P}_p\omega_s\omega_i}{\pi\varepsilon_0c^3n_sn_pn_i}\frac{\mathscr{L}^2}{A_I}\mathrm{sinc}^2\left(\frac{\Delta k\mathscr{L}}{2}\right)d\omega_s \tag{15}$$

#82210 - $15.00 USD Received 18 Apr 2007; revised 24 May 2007; accepted 31 May 2007; published 4 Jun 2007
(C) 2007 OSA

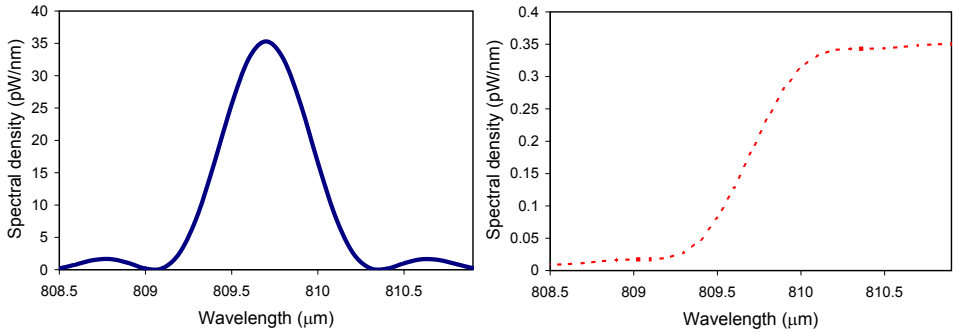

Fig. 1. Signal power densities for waveguides (left plot) and bulk (right plot). The densities are calculated for a 1 mW pump laser. Notice the different vertical scales for the two plots.

Finally the down-converted signal power $d\mathscr{P}_s^{(W)} = \hbar\omega_s \mathscr{W}$ emitted in a frequency or wavelength interval is

$$d\mathscr{P}_s^{(W)} = \frac{\hbar d^2 \omega_s^2 \omega_i \mathscr{L}^2 \mathscr{P}_p}{\pi c^3 \varepsilon_0 n_s n_i n_p A_I} \mathrm{sinc}^2\left(\frac{\Delta k \mathscr{L}}{2}\right) d\omega_s = \frac{16\pi^3 \hbar d^2 \mathscr{L}^2 c \mathscr{P}_p}{\varepsilon_0 n_s n_i n_p \lambda_s^4 \lambda_i A_I} \mathrm{sinc}^2\left(\frac{\Delta k \mathscr{L}}{2}\right) d\lambda_s \quad (16)$$

Figure 1 shows a comparison of the expected spectral power densities $\frac{d\mathscr{P}_s^{(W)}}{d\lambda_s}$ and $\frac{d\mathscr{P}_s^{(B)}}{d\lambda_s}$ for waveguide and bulk, respectively. To obtain the curves we have assumed type II degenerate SPDC in periodically poled potassium titanyl phosphate (PPKTP) with a 404.85 nm pump. In the simulation as well as in the experiments the pump is polarized along the crystallographic $\hat{Y}$ axis, signal and idler are polarized along the $\hat{Y}$ and $\hat{Z}$ axes, respectively, and all beams propagate along the $\hat{X}$ axis. The relevant nonlinear coefficient is $d = 2d_{24}/\pi$ where $d_{24} = 3.92$ pm/V [11] and the factor $2/\pi$ is due to the first-order poling. We also put $\mathscr{L} = 10$ mm, $\lambda_p = \frac{\lambda_s}{2} = \frac{\lambda_i}{2} =$ 404.85 nm, $n_s = 1.758$, $n_i = 1.843$, $n_p = 1.840$, and $\mathscr{P}_p = 1$ mW. Finally we assume

$$\Delta k \equiv \beta_p - \beta_s - \beta_i - \frac{2\pi}{\Lambda} = k_p - k_s - k_i - \frac{2\pi}{\Lambda} + \Delta k_{WG}, \quad (17)$$

where we have introduced the factor $2\pi/\Lambda$ to take into account the effect of the poling grating of period $\Lambda = 8.36\ \mu$m for the waveguide and $\Lambda = 10\ \mu$m for the bulk crystal. To evaluate Δk we use the pump, signal, and idler wave numbers $k_{p,s,i}$ and the waveguide contribution to the phase matching Δk_{WG}. The latter factor has been evaluated empirically to be $\Delta k_{WG} \sim 0.13\ \mu\mathrm{m}^{-1}$. The dependence of the wave numbers on the wavelengths can be evaluated using the Sellmeier equations for KTP [12]. Finally we use $A_I = 15\mu\mathrm{m}^2$ as calculated from the waveguide eigenmodes which will be derived in the next section.

Let us sum up here the differences between our approach and the one used for bulk crystals in Ref. [8]. The main difference is that in the waveguide only 3 modes effectively interact while in the bulk the pump gaussian mode interacts with a continuum of plane-wave modes. This changes both the density of states and the overlap integrals of the modes. These differences are mirrored by the differences that emerge from a comparison of Eqs. 1 and 16 represented in Fig. 1. The waveguide emission is confined to a limited band due to the sinc term whereas Eq. 1 predicts that far from collinear emission the bulk spectral density is almost flat as experimentally verified in Ref. [13]. This difference is due to the fact that the waveguide down-conversion is essentially a 1 dimensional problem while the bulk has to be treated as a 3 dimensional problem

#82210 - $15.00 USD Received 18 Apr 2007; revised 24 May 2007; accepted 31 May 2007; published 4 Jun 2007
(C) 2007 OSA

(because one has to consider the interaction of the pump with all plane waves). The resulting effect is not dissimilar from the spectral redistribution observed in SPDC experiments inside cavities [14]. It is also apparent that waveguide emission is much more brilliant than the bulk. We attribute this to two interrelated effects: the spectral redistribution mentioned before and the ability of the waveguide to enhance SPDC by increasing mode overlap between the pump, signal, and idler. It is also significant that the spectral density in the waveguide depends on $\mathscr{L}^2$ whereas in the bulk it depends on $\mathscr{L}$. Notice however that in the waveguide, as the crystal length increases, the width of the spectrum decreases. Because of this the power integrated over the whole emission spectrum grows linearly with $\mathscr{L}$.

The expected number of pairs generated by the bulk crystal and the waveguide can be estimated using Eq. 1 and 16. If we limit the detection window using a 1-nm FWHM gaussian filter centered around the degenerate frequency we obtain an estimated pair flux of $\sim 7.6 \cdot 10^7$ pairs/s per mW of pump for the waveguide and $\sim 1.6 \cdot 10^6$ pairs/s for the bulk.

3. Waveguide fabrication

The PPKTP waveguides are fabricated using photolithography on a flux grown, z-cut KTP wafer. A direct contact mask designed for 4 μm wide channel waveguides is used to pattern a layer of Al onto the +z surface of the wafer. The wafer is diced into 3 mm x 10 mm chips and polished on the optical surfaces. The chips are placed in a molten bath of $RbNO_3$ salt at 400C for 120 minutes. The bare areas of the patterned surface undergo ion exchange in which Rb^+ ions diffuse into the KTP, replacing K^+ ions to a depth of around 9 μm, forming an index step of 0.02 relative to the surrounding KTP. After ion exchange the Al layer is removed, and the chip is annealed in air at 325°C for 15 minutes.

We use a finite difference scalar approximation to calculate the eigenmodes of the waveguide [15]. The index distribution is described by a step profile of width 4 μm in the lateral direction and a diffusion profile as a function of depth z of the form $n(z) = n_{KTP} + \Delta n e^{(-z/d)}$, with $\Delta n = 0.02$ and $d = 8\mu$m [16]. The fundamental modes of the waveguide are shown in Fig. 2. Using the electric field distributions so calculated we obtain the estimate for A_I used above.

The waveguides were periodically poled using an electrode on a separate glass substrate placed in contact with the KTP surface. The electrode was fabricated using contact lithography to define a chrome grating pattern with a period of 8.36 μm. The patterned electrode was aligned and pressed to the +z surface; a ground electrode consisting of a uniform metal substrate contacted the -z surface. The poling waveform was applied using a Trek 20/20C high voltage amplifier controlled by a computer program that simultaneously monitored the electrode current.

4. Experiments

A schematic of the experimental setup used to test the down-conversion in the waveguides and bulk crystals is shown in Fig. 3. We use a grating-stabilized cw laser diode with an emission wavelength of 404.85 nm. The laser is coupled into one of the waveguides on the PPKTP chip using an aspheric lens. The optimized transmission of the 404.85 nm pump through the waveguide is 36%. Using second harmonic generation we verified that the waveguides can phase match degenerate type-II down-conversion at the pump wavelength at a temperature of approximately 18° C.

The output of the waveguide is collimated with a second aspheric lens and the residual pump is filtered with a dichroic mirror. In some of the experiments the output is filtered further using a 1-nm bandpass interference filter nominally centered at 810 nm. The filter can be slightly angle-tuned to optimize transmission of the degenerate down-converted pairs. After filtering we send the pairs to a polarization beam splitter that separates signal and idler photons. Finally

#82210 - $15.00 USD Received 18 Apr 2007; revised 24 May 2007; accepted 31 May 2007; published 4 Jun 2007
(C) 2007 OSA

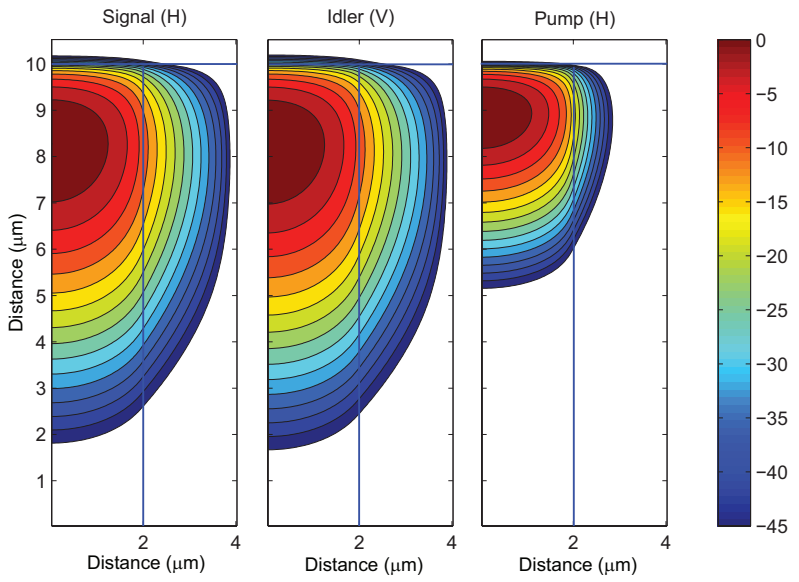

Fig. 2. Intensity plot of the eigennmodes for the signal, idler, and pump. The blue lines indicate the edge of the crystal (top) and the edge of the diffusion profile zone (center). Only half of the structure has to be simulated given the problem symmetry. The scale is in dB and is normalized to the peak intensity. A finite difference scalar approximation was used to solve the eigenmode problem.

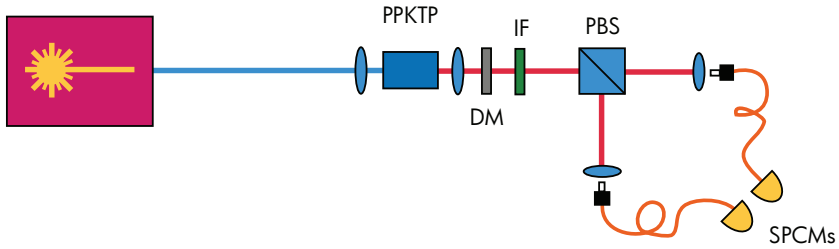

Fig. 3. Experimental setup for waveguide test. PPKTP, periodically poled crystal with waveguides; DM, dichroic mirror reflects 405 nm transmits 810 nm; IF, interference filter at 810 nm 1 nm FWHM; PBS, polarization beam splitter; SPCMs; single photon counting modules.

the down-converted photons are coupled into multimode fibers for detection and analysis. The pairs are detected using two single-photon detection modules and a home-made coincidence detector [17] with a coincidence window of 3.2 ns.

In Fig. 4 we show the spectrum of the signal photons obtained using a spectrometer with a 1200 lines/mm grating and a cooled CCD detector. In the spectrum we observe two emission peaks: we attribute the two peaks to the phase matching of two separate pump spatial modes. Multiple peaks in second harmonic generation have been observed previously [16] in periodically poled waveguides. The intensity in the large peak has been optimized by changing the coupling lens system and alignment. A fit of the peak with a sinc^2 curve yields a FWHM of 0.65 nm which should be compared with the expected width of 0.57 nm calculated using Eq. 16. A possible explanation of the difference between the expected and calculated width is that

#82210 - $15.00 USD Received 18 Apr 2007; revised 24 May 2007; accepted 31 May 2007; published 4 Jun 2007
(C) 2007 OSA

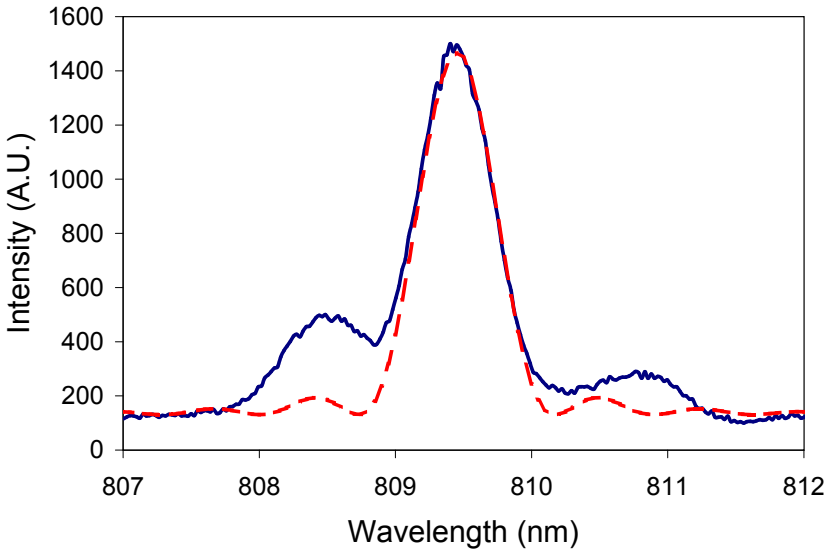

Fig. 4. Measured spectrum for the signal (horizontally polarized) down-converted beam (blue continuous curve) with a sinc^2 fit to the data (red dotted curve), background has been subtracted. To obtain the spectrum 20 mW of pump were used.

the crystal length that is effectively poled is shorter than the physical length of the crystal due to imperfections in the poling process.

The spectrum also shows a pedestal which we attribute to fluorescence photons generated in the crystal. The large number of fluorescence photons in down-conversion experiments in waveguides has been reported by U'ren and co workers [6]. In that paper the authors used an ultrafast laser pump and were therefore able to temporally resolve the fast down-conversion pair emission from the slow (lifetime >1 ns) fluorescence emission. They estimate a 1:1 ratio of down-converted to fluorescence photons. In our experiment we use a cw pump and therefore we cannot temporally resolve the fluorescence photons. We can, however, estimate the fluorescence photons from the spectrum in Fig. 4. To do so we calculate the area of the sinc^2 peak and compare it to the area of pedestal under it. We obtain a 4:1 ratio of down-converted to fluorescence photons. The down-converted photons are spectrally confined in a 1-nm band while the fluorescence photons are spread all over the spectrum. It is therefore convenient to use a 1-nm interference filter to limit the number of fluorescence photons detected. For a transmitted pump of 12 μW (33 μW injected) with a 1-nm filter we measure $N_s = 209,000$ signal counts/s, $N_i = 218,000$ idler counts/s, and $N_c = 35,000$ coincidence counts/s. This corresponds to $2.9 \cdot 10^6$ pairs/s per mW of transmitted pump ($9.7 \cdot 10^5$ pairs/s per mW of injected pump). If 20% of the singles counts is caused by fluorescence photons as shown before, we obtain an estimate of the detection and collection efficiencies $\eta_s \simeq \eta_i \simeq 0.2$. Using this estimate of the losses in the detection system we calculate a generation rate of $\sim 7.3 \cdot 10^7$ pairs/s per mW of transmitted pump. This value should be compared with the expected pair generation rate of $7.6 \cdot 10^7$ pairs/s per mW. The discrepancy between the measured and calculated values can be due to a number of factors. We have neglected the effects of pump coupling into modes other than the fundamental that effectively reduces the available power. Moreover imperfections in the poling might reduce the effective nonlinear coefficient and interaction length.

We also compare waveguide rates with those measured in an experiment that used a bulk crystal. For this experiment the setup of Fig. 3 is modified by substituting the waveguide chip

#82210 - $15.00 USD Received 18 Apr 2007; revised 24 May 2007; accepted 31 May 2007; published 4 Jun 2007
(C) 2007 OSA

with a bulk PPKTP crystal. The crystal is 1x2x10 mm^3 and has a poling period of 10 μm that phase matches degenerate type II down-conversion of a pump at 404.85 nm. The second aspheric lens is moved to optimize coupling into the multimode fibers. Given the large numerical aperture of the aspheric lens and the relatively narrow emission cone of the pairs (for the bandwidth we consider) it can be safely assumed that all pairs generated in the band of interest are collected. For a transmitted pump of 440 μW (810 μW injected) with a 1-nm filter we measure $N_s = 149,000$ signal counts, $N_i = 165,000$ idler counts, and $N_c = 24,000$ coincidence counts, this corresponds to a rate of 54,000 pairs/s/mW/nm. By changing the crystal temperature we obtain an estimate of the fluorescence photons for the two channels $N_{fs} = 17,000$ counts/s and $N_{fi} = 16,500$ counts/s, this corresponds to a 9:1 ratio between down-converted and fluorescence photons. Using these numbers we estimate detection and collection efficiencies $\eta_s = 0.18$ and $\eta_s = 0.16$ and an estimated generation rate of $1.8 \cdot 10^6$ pairs/s/mW in the filter band which is in qualitative agreement with the expected value of $1.5 \cdot 10^6$ pairs/s/mW. The discrepancy is most likely due to our rough estimate of the fluorescence photons. For our experiments the measured pair rate in the waveguide is approximately 50 times larger than the bulk in a 1-nm band.

The pair rate we observed in the waveguide also compares favorably with the rates obtained by other groups. Ref. [4] reports a rate of 1500 pairs/s for 1 μW of pump in a 30-nm bandwidth corresponding to 50,000 pairs/s/mW in a 1 nm band or $1.5 \cdot 10^6$ pairs/s/mW in the aggregate band. Because of the wavelength used Ref. [4] has a much lower detection efficiency than our experiment. However Ref. [4] used type I SPDC in periodically poled Lithium Niobate that has a much larger nonlinear coefficient than PPKTP. Reference [6] reports a rate of 2500 pairs/s for 3 μW pump [18] in a 17-nm bandwidth corresponding to 50,000 pairs/s/mW in a 1 nm band or $8.5 \cdot 10^5$ pairs/s/mW in the aggregate band.

We perform a quantum interference experiment to measure the indistinguishability of the photon generated in the waveguide using a setup similar to the one described in Ref. [19]. A 5 mm KTP crystal with its optical axis perpendicular to the PPKTP crystal is added between the second lens and the filters to compensate the delay due to the PPKTP birefringence. We add a half-wave plate that allows us to rotate the polarization of signal and idler photons and clean-up polarizers in front of the fiber couplers. Rotating the half-wave plate reveals interference fringes in the coincidence counts that have perfect visibility for indistinguishable photons. This experiment is equivalent to the Hong-Ou-Mandel interferometer [20]. We measure the maxima $N_c^{(max)}$ and minima $N_c^{(min)}$ of the interference fringes to obtain a visibility $V = (N_c^{(max)} - N_c^{(min)})/(N_c^{(max)} + N_c^{(min)}) = 79\%$. We attribute the imperfect visibility to a spatial mode mismatch of the signal and idler photons.

5. Conclusions

In this paper we have described an experiment of generation of correlated pairs using SPDC in PPKTP waveguides. We measured a pair rate of $2.9 \cdot 10^6$ pairs/s/mW for a 1 nm bandwidth that greatly exceeds the rate measured for a bulk crystal. In a theoretical analysis we show that the difference in the rates is shown to be due to a spectral redistribution of the photon pairs generated in the waveguide and field overlap enhancement due to the confinement. A qualitative agreement between the theory and experiment is obtained. We have found that this waveguide has an higher number of fluorescence photons than what was found in a bulk PPKTP sample (which was obtained from a different vendor). Further work is need to resolve whether the increase is due to the waveguide manufacturing process, the larger collection efficiency of the waveguide, or because the KTP substrates used were from two different manufacturers.

The high-rate pair source presented here can be integrated to build chip-scale sources of polarization-entangled photons with applications in practical quantum key distribution and quantum information processing.

#82210 - $15.00 USD Received 18 Apr 2007; revised 24 May 2007; accepted 31 May 2007; published 4 Jun 2007
(C) 2007 OSA

This work was supported in part by the Disruptive Technology Office under contract NBCHC060076. We thank Franco N.C. Wong for useful discussions.

#82210 - $15.00 USD Received 18 Apr 2007; revised 24 May 2007; accepted 31 May 2007; published 4 Jun 2007
(C) 2007 OSA

80.110.78.245 (ts '2019-07-08 09:20:03')